Title

Intraoperative Mapping of Parathyroid Glands using Fluorescence Lifetime Imaging

Authors

Marsden, Mark
Weaver, Shamira Sridharan
Marcu, Laura
et al.

Publication Date

2021-09-01

DOI

10.1016/j.jss.2021.03.023

Peer reviewed

HHS Public Access

Author manuscript

J Surg Res. Author manuscript; available in PMC 2022 September 01.

Published in final edited form as:

J Surg Res. 2021 September ; 265: 42–48. doi:10.1016/j.jss.2021.03.023.

Intraoperative Mapping of Parathyroid Glands using Fluorescence Lifetime Imaging

Mark Marsden, Ph. D.,
University of California, Davis Department of Biomedical Engineering

Shamira Sridharan Weaver, Ph. D.,
University of California, Davis Department of Biomedical Engineering

Laura Marcu, Ph. D.,
University of California, Davis Department of Biomedical Engineering

Michael J. Campbell, MD
University of California, Davis Department of Surgery

Abstract

Background—Hypoparathyroidism is a common complication following thyroidectomy. There is a need for technology to aid surgeons in identifying the parathyroid glands. In contrast to near infrared technologies, fluorescence lifetime imaging (FLIm) is not affected by ambient light and may be valuable in identifying parathyroid tissue, but has never been evaluated in this capacity.

Methods—We used FLIm to measure the UV induced (355 nm) time-resolved autofluorescence signatures (average lifetimes in 3 spectral emission channels) of thyroid, parathyroid, lymphoid and adipose tissue in 21 patients undergoing thyroid and parathyroid surgery. The Mann-Whitney U test was used to assess the ability of FLIm to discriminate normocellular parathyroid from each of the other tissues. Various machine learning classifiers (random forests, neural network, support vector machine) were then evaluated to recognize parathyroid through a leave-one-out cross-validation.

Results—Statistically significant differences in average lifetime were observed between parathyroid and each of the other tissue types in spectral channels 2 and 3 respectively. The largest change was observed between adipose tissue and parathyroid ($p<0.001$), while less pronounced but still significant changes were observed when comparing parathyroid with lymphoid tissue ($p<0.05$) and thyroid ($p<0.01$). A random forest classifier trained on average lifetimes was found to detect parathyroid tissue with 100% sensitivity and 93% specificity at the acquisition run level.

Corresponding Author: Michael J Campbell, MD, University of California, Davis, Comprehensive Cancer Center, 4501 X St., Sacramento, CA 95817, Phone: 916-734-9507, Fax: 916-734-7417, mjcampb@ucdavis.edu.

SSW, LM, MJC were involved in study conception and design, SSW, MJC were involved in data acquisition, MM, LM, MJC were involved in analysis and interpretation of data, SSW, MM, MJC, LM were involved in drafting the manuscript.

The authors have no conflicts of interest to disclose. Department funds were used for incidental expenses

Conclusion—We found that FLIm derived parameters can distinguish the parathyroid glands and other adjacent tissue types and has promise in scanning the surgical field to identify parathyroid tissue in real-time.

Keywords

Hypoparathyroidism; parathyroid identification; fluorescence lifetime imaging

Introduction

Thyroidectomy is a common procedure with 72,344 operations performed in the United States in 2011[1] .Hypoparathyroidism, or dysfunction of the parathyroid glands leading to hypocalcemia, is a frequent complication of thyroidectomy occurring in approximately 10% of patients who undergo thyroid procedures[2]. Even among high-volume thyroid surgeons, up to 3% of patients will develop permanent hypoparathyroidism leading to lifelong replacement with calcium and vitamin D[3]. The cost of caring for patients with hypoparathyroidism is estimated to be three times that of a healthy patient[4]. Currently, the majority of thyroid operations in the United States are performed by low-volume surgeons[5]. The effectiveness of surgeon identification and preservation of the parathyroid glands varies by surgeon experience with low-volume surgeons having increased rates of both temporary and permanent hypoparathyroidism[6]. The current standard for identifying and protecting the parathyroid glands is visual identification of the glands. Unfortunately, the parathyroid glands' small size and nondescript nature make them easily confused for thyroid tissue, lymph nodes or even benign fat. There is a need for technology to aid surgeons, especially low-volume surgeons, in the identification and confirmation of the parathyroid glands during thyroid surgery that can help lead to more consistent surgical outcomes.

In 2011, Parras et al.[7] introduced the novel technique of near infrared detection for intraoperative parathyroid identification. This was followed in 2013 with a similar method by McWade et al.. In 2014, McWade et al. [9] then introduced the feasibility of NIR imaging for intraoperative parathyroid identification using a modified Karl Storz camera. Since 2014, additional studies have supported these findings that NIR fluorescence can aid in the detection of parathyroid tissue during thyroid surgery[10,11]. Early studies using NIR fluorescence imaging allowed surgeons to scan the operative field for parathyroid tissue using a camera with a 25 cm^2 field of view, but relied on the operating room (OR) lights being turned off because of interference between ambient light and the light emitted from intrinsic parathyroid fluorophores in the NIR optical window . More recent studies using NIR fluorescence imaging have advanced the technology to be able to take point measurements of tissue in the prsesense of ambient OR lighting, but NIR technology still cannot aid in spatially mapping the parathyroids within the surgical field without redirecting or turing off the OR spot lights [12]. The next logical step is to develop a technology which allows surgeons to scan the operative field with a large field of view for parathyroid tissue while leaving the OR lights on to minimize disruptions.

Multispectral fiber-based fluorescence lifetime imaging (FLIm) is a novel technique using a handheld laser induced fluorescence probe to record and measure spectroscopic differences

between various tissue types. Unlike NIR fluorescence imaging, FLIm measures the autofluorescence signature of tissue in the visible spectrum following ultraviolet (UV) excitation and does not require the administration of an exogenous contrast agent. The pulsed operation of FLIm detection makes it insensitive to OR lights. This approach enables scanning of the surgical field to identify parathyroid tissue without the disruption of turning off or redirecting the the OR spot lights. The purpose of this pilot study is to evaluate the ability of FLIm to identify parathyroid tissue in patients undergoing thyroid and parathyroid surgery.

Methods

The study was conducted on 21 patients undergoing thyroid and parathyroid surgery following informed consent under the University of California Davis institutional review board approval. The use of FLIm in the OR did not change the general flow of the thyroid and parathyroid surgery. A single, high volume endocrine surgeon (MJC) identified each patient's parathyroid glands based on their visual appearance and anatomic location. As each parathyroid was identified, a sterilized fiberoptic probe was brought into the operative room and connected to the FLIm instrumentation. Optical measurements of the parathyroid gland were taken, as well as the adjacent thyroid, lymph node and adipose tissue. The location of these measurements was guided through the use of an endoscopic camera. The surgeon was blinded to these results, with all analysis and classification performed post-hoc in this pilot study. As it would be unethical to remove or biopsy parathyroid tissue for research purposes, the surgeon filled out a standardized assessment of his confidence that he correctly identified the parathyroid gland as he identified each gland. Only data collected on parathyroid glands identified by the surgeon with a high level of confidence and felt to be normal sized and non-hypercellular were included in analysis for this study.

The FLIm instrumentation

The FLIm system has been described in detail previously[13-15]. Briefly, the FLIm system uses a 355 nm pulsed (600 ps pulse width and 2.5 μJ per pulse) laser light source coupled to a fiber optic (400 μm core diameter) to excite native fluorophores in tissue. The fluorescence emission is collected using the same fiber and spectrally resolved into three spectral channels: 390±20 nm, 470±14 nm, and 542±25 nm. These spectral band target the reported autofluorescence emission maxima of the following endogenous fluorphores: (CH1: collagen, CH2: nicotinamide adenine dinucleotide (NADH), CH3: flavin adenine dinucleotide (FAD))[15]. The FLIm apparatus used allows for the recording of data in a fourth channel (629±26 nm); however, signal intensity in this channel was observed to be very weak for several tissue conditions in this specific study, resulting in a low signal-to-noise ratio (SNR). Therefore, this channel was not used for analysis in this case but has been in other studies. Average fluorescence lifetime for each channel was retrieved using a Laguerre expansion deconvolution of the recorded intensity decay at each measurement point[16]. The diagnostic contrast provided by these time-resolved spectroscopic parameters for the task of parathyroid identification was investigated in this study. Additionally, a blue aiming beam (445 nm) coupled to the same fiber optic used to induce/collect tissue autofluorescence and captured using a laparoscopic camera was used to identify the spatial location of

fluorescence point-measurements. This method was described previously by our group[17,18] and allows for point-measurement localization and the generation of fluorescence parametric maps that are then overlaid directly onto white light images of the tissue surface (see figure 1). The RF amplifier of the instrument was AC coupled with a cut off frequency of 10 kHz in order to filter out any signal contribution from the aiming beam and operating room lights as described previously[17].The average spatial resolution of a manual scan using FLIm is 60 points/mm^2 [19]. The power being delivered to tissue was 2.2-2.6 mW.

The measurements in this study involve multiple repetitions: there are 300-1200 data points for each tissue type from each patient. The goal was to acquire as much data as possible within each surgical procedure to perform statistical analysis and machine learning. In practice, fewer point-measurements (~100) would be sufficient to perform a highly robust prediction for a given tissue location with a trained machine learning model. The Shapiro-Wilk normality test[20] was used to decide whether parametric statistical tests should be used for this study. The application of this test demonstrated a non-normal distribution within the acquired average fluorescence lifetime values, therefore the nonparametric Mann-Whitney U-test[21] was used to compare tissue types. A statistical power analysis was performed using the statsmodel python library (effect size=1.0, statistical power=0.8, p value=0.05), calculating a sample size of N=16 for patient level comparisons between groups. For each subject the median was calculated for each FLIm parameter for all tissue types. These median values were then used to compare tissues across the full dataset. Statistical analysis was performed using Graphpad Prism 8.

Average fluorescence lifetimes calculated from three channels for each data point were used to train a machine learning classifier for the identification of parathyroid glands. To evaluate the classification method, a leave-one-out cross-validation approach was performed in which data from one patient was removed for each fold and tested on while training with the other patients before repeating for all patients and calculating mean performance. Classification performance was evaluated at the point-measurement level and at the acquistion run level (with a single mean prediction calculated for all points within a run). A given acquisiton run repeatedly measures a specific tissue region to determine if this tissue is parathyroid, making it appropriate to calculate a single classification output at the run level for this application. Three machine learning classifiers were evaluated (random forests[22], neural network[23], support vector machine[24]) using the Scikit-learn Python package. An overview of this FLIm-based classification pipeline is presented in figure 2.

Results

Twenty-one patients undergoing thyroid and parathyroid surgery were included in our study. The mean age was 55.6 years (range: 35-74 years). Eighteen (86%) patients were women. Thirteen patients (62%) had a hemi- or total thyroidectomy, 7 (33%) had a parathyroidectomy and 1 (5%) had both a thyroidectomy and parathyroidectomy. Of the patients undergoing a thyroidectomy 7 (33%) had benign disease and 3 (14%) had evidence of autoimmune thyroiditis on their surgical pathology. Following the removal of low confidence and high-cellularity parathyroid runs, 29393 point-measurements from 15 patient remained for the analysis stage, with parathyroid and at least two of the other tissues imaged

for all patients. From these 15 patients, 15 parathyroid samples, 15 thyroid samples, 9 lymph node samples and 15 adipose tissue samples were imaged.

Significant differences in average fluorescence lifetime were observed between parathyroid and each of the other tissue types in spectral channels 2 and 3 (see figure 3). The largest change was observed between adipose tissue and parathyroid ($p<0.001$), while less pronounced but still significant changes were observed when comparing parathyroid with lymphoid tissue ($p<0.05$) and thyroid ($p<0.01$). Parathyroid has the shortest average lifetime of all tissue types in channels 2 and 3, while adipose tissue has the longest average lifetime in channels 2 and 3.

Tables 1 and 2 present classification performance at the point-measurement and run level for a 15-patient cross validation. The random forest classifier was observed to achieve superior sensitivity for both evaluations. Figure 4 presents ROC curves calculated at point-measurement level for each patient using the random forests method. A mean patient level AUC of 0.88±0.08 was observed at the point-measurement level, with the lower AUC cases attributed to lymphoid tissue occasionally being misclassified as parathyroid. Performance at the run-level is noticeably higher due to the aggregation of points within a run, alleviating local variation between measurements, with 100% sensitivity and 93% specificity observed using the random forest method across 41 runs. This corresponds to an overall run-level accuracy of 97% and is representative of the proposed use case. All false positives at the run-level were also attributed to lymphoid tissue.

Discussion

Protection of the parathyroid glands and their blood supply are important elements of successful thyroid surgery. Unfortunately, unintentional damage to the parathyroid glands is common even in the hands of experienced endocrine surgeons. In this study we found that times-resolved FLIm can be successfully used to distinguish parathyroid glands from thyroid, adipose and lymph tissue without the disruption of turning off or redirecting the OR lights. This builds on the weakness of previous technologies and could potentially allow for future integration into visual augmentation schemes where surgeons can use FLIm data overlaid on real-time images of the operative field to identify and confirm parathyroid tissue.

We found significant differences in average fluorescence lifetimes when parathyroid was compared with thyroid, lymphoid and adipose tissue respectively. These changes were observed in spectral channels 2 and 3 of the FLIm instrument, both of which are linked with metabolic activity. The extent of this contrast varies between tissue types, with the largest difference observed for adipose tissue, which shows noticably longer lifetimes in CH2 and CH3. Adipose tissue has previously been shown to have long fluorescence lifetimes at higher wavelengths, specifically for breast specimens imaged *ex vivo* using the same FLIm instrument [19]. This increase in lifetime at higher wavelengths for adipose tissue has been observed to be a result of lipid oxidation[25] and is consistent with previous studies[26]. Higher variance was also observed in the fluorescence lifetimes of lymph nodes, resulting in rare false positives for this tissue type. Various factors can contribute to this variation between patients. One such source of variation is the fact that lymphocytes constitute the majority of

the lymph node architecture and this may lead to low autofluorescence signal due to a high nucleus to cytoplasm ratio[27] in certain cases. Conversley, hyperplasia in the lymph node, which may occur secondary to inflammation, can lead to an increase in NADH, potentially leading to higher fluorescence contributions in Channel 2 for other patients.

The random forests classifier method achieves strong sensitivity for parathyroid detection. Similarly accurate discrimination of tissue conditions was observed using random forests in prior FLIm studies on breast cancer detection in excised specimens[28] and intraoperative head and neck cancer detection[29]. The ensemble approach of random forests allows for this method to avoid model overfitting by combining the output of 100 decision tree classifiers to form an aggregate prediction. The other methods investigated (SVM, neural network) do not apply this aggregation step and fail to overcome the variability between FLIm point-measurments for a given tissue condition and the variability between tissue conditions in the negative class (adipose, thyroid, lymphoid). This difference is more prounounced at the run level, where greater consistency between predictions is required. Another key advantage of the random forest method is its high computational efficiency which makes it suitable for real-time applications.

Various NIR light source based wide-field imaging techniques have been studied for parathyroid gland identification with success[10,30,31]. However, due to the effects of ambient light on collected signals, these techniques require OR lights to be turned off or re-directed which can be disruptive to surgical workflow. To overcome this short coming, the PT Eye instrument allows for the taking of point measurements to identify parathyroid tissue by a surgical team without disruption of the ambient OR lights[12]. The reported accuracy of the intensity-based PT Eye instrument for parathyroid identification is 96.1% compared to the 97% detection accuracy achieved using FLIm. However, due to the limited measurement spot size of 400 μm, signal acquisition time of 2 seconds (300 ms integration time) and the need for a 10 second calibration step, PT Eye is better suited for situations where the surgeon has an a priori suspicion of a tissue region being parathyroid[12]. FLIm on the other hand is capable of rapid signal integration (<30 ms per data point) without the need for an initial calibration step to establish a baseline for thyroid. This rapid signal integration time allows for more tissue regions to be investigated within a time constrained procedure. Another recent NIR based approach is the Fluobeam LX[32], which is shown to be robust to ambient lighting but still requires the OR spot lights to be redirected. The developed FLIm method shows great potential to address the key challenges of both PT Eye and Fluobeam if implemented into a real-time parathyroid detection system.

Our study presents a novel solution to one of the current problems encountered by NIR technologies for identifiying parathyroid tissue during thyroid surgery, but it does have several limitations. This current study was performed using surgical decisions made by a single experienced endocrine surgeon. Future projects would benefit from including several surgeons, in multiple institutions, to study the effects of inter-observer variability on classification accuracy. While this study focuses on the detection of normocellular parathyroid, future work will look to expand on this initial proof of concept approach and allow for various parathyroid conditions (e.g. parathyroid adenoma, parathyroid hyperplasia, vascularized and devascularized parathyroid) to be detected through the acquisition of a

larger and more varied dataset. Future developments will allow for implementation of an algorithm to allow for online, real-time tissue classification (>30 frames per second) that can be augmented on the surgical field of view to assist surgeons during thyroid and parathyroid surgery. A real-time visualization will be produced that can present classifier output to the surgeon by augmenting the video stream of a handheld surgical camera. This approach will be developed by adapted an existing fluorescence imaging visualization method that has been demonstrated for intraoperative head and neck cancer detection[18].

Conclusion

Current results demonstate that FLIm has a good sensitivity and specificity for the rapid identification of parathyroid tissue in patients undergoing thyroid and parathyroid operations, without turning off or redirecting the OR lights. Thus, FLIm has the potential to be a useful adjunct to identifying parathyroid tissue in patients undergoing thyroid surgery.

Acknowledgements

The authors acknowledge Julien Bec for his contributions to adaptation of the system hardware for clinical use cases. The authors would also like to acknowledge Hannah Kim and Jakob Unger for their assistance with the clinical acquisition and preparation of FLIm data.

Disclosure

The project described was supported by the National Institutes of Health [grant number NIH R01 CA187427]. Additional funds were provided by the American Cancer Society and the Dean of School of Medicine [grant number ACS IRG-95-125-13]. The authors report no proprietary or commercial interest in any product mentioned or concept discussed in this article.

References

1. Sosa JA, Hanna JW, Robinson KA, Lanman RB. Increases in thyroid nodule fine-needle aspirations, operations, and diagnoses of thyroid cancer in the United States. Surgery. 2013;154(6):1420–1427. [PubMed: 24094448]
2. Rosato L, Avenia N, Bernante P, et al. Complications of thyroid surgery: analysis of a multicentric study on 14,934 patients operated on in Italy over 5 years. World J Surg. 2004;28(3):271–276. [PubMed: 14961204]
3. Zarnegar R, Brunaud L, Clark OH. Prevention, evaluation, and management of complications following thyroidectomy for thyroid carcinoma. Endocrinol Metab Clin. 2003;32(2):483–502.
4. Clarke BL, Brown EM, Collins MT, et al. Epidemiology and diagnosis of hypoparathyroidism. J Clin Endocrinol Metab. 2016;101(6):2284–2299. [PubMed: 26943720]
5. Lorente-Poch L, Sancho JJ, Ruiz S, Sitges-Serra A. Importance of in situ preservation of parathyroid glands during total thyroidectomy. Br J Surg. 2015. doi:10.1002/bjs.9676
6. Adam MA, Thomas S, Youngwirth L, et al. Is there a minimum number of thyroidectomies a surgeon should perform to optimize patient outcomes? Ann Surg. 2017;265(2):402–407. [PubMed: 28059969]
7. Paras C, Keller M, Mahadevan-Jansen A, White L, Phay J. Near-infrared autofluorescence for the detection of parathyroid glands. J Biomed Opt. 2011;16(6):67012.
8. McWade MA, Paras C, White LM, Phay JE, Mahadevan-Jansen A, Broome JT. A novel optical approach to intraoperative detection of parathyroid glands. Surgery. 2013;154(6):1371–1377. [PubMed: 24238054]
9. McWade MA, Paras C, White LM, et al. Label-free intraoperative parathyroid localization with near-infrared autofluorescence imaging. J Clin Endocrinol Metab. 2014;99(12):4574–4580. [PubMed: 25148235]

10. Falco J, Dip F, Quadri P, de la Fuente M, Rosenthal R. Cutting edge in thyroid surgery: autofluorescence of parathyroid glands. J Am Coll Surg. 2016;223(2):374–380. [PubMed: 27212004]
11. Kim SW, Lee HS, Ahn Y-C, et al. Near-infrared autofluorescence image-guided parathyroid gland mapping in thyroidectomy. J Am Coll Surg. 2018;226(2):165–172. [PubMed: 29122718]
12. Thomas G, McWade MA, Paras C, et al. Developing a clinical prototype to guide surgeons for intraoperative label-free identification of parathyroid glands in real-time. Thyroid. 8 2018. doi:10.1089/thy.2017.0716
13. Ma D, Bec J, Gorpas D, Yankelevich D, Marcu L. Technique for real-time tissue characterization based on scanning multispectral fluorescence lifetime spectroscopy (ms-TRFS). Biomed Opt Express. 2015;6(3):987–1002. doi:10.1364/boe.6.000987 [PubMed: 25798320]
14. Weyers BW, Marsden M, Sun T, et al. Fluorescence Lifetime Imaging (FLIm) for Intraoperative Cancer Delineation in Transoral Robotic Surgery (TORS). Transl Biophotonics. 10 2019. doi:10.1002/tbio.201900017
15. Yankelevich DR, Ma D, Liu J, et al. Design and evaluation of a device for fast multispectral time-resolved fluorescence spectroscopy and imaging. Rev Sci Instrum. 2014;85(3). doi:10.1063/1.4869037
16. Liu J, Sun Y, Qi J, Marcu L. A novel method for fast and robust estimation of fluorescence decay dynamics using constrained least-squares deconvolution with Laguerre expansion. Phys Med Biol. 2012;57:843–865. doi:10.1088/0031-9155/57/4/843 [PubMed: 22290334]
17. Gorpas D, Ma D, Bec J, Yankelevich DR, Marcu L. Real-Time Visualization of Tissue Surface Biochemical Features Derived from Fluorescence Lifetime Measurements. IEEE Trans Med Imaging. 2016;35:1802–1811. doi:10.1109/tmi.2016.2530621 [PubMed: 26890641]
18. Marsden M, Fukazawa T, Deng Y-C, et al. FLImBrush: Dynamic Visualization of Intraoperative Free-hand Fiber-based Fluorescence Lifetime Imaging. Biomed Opt Express. 2020;11(9):5166–5180. [PubMed: 33014606]
19. Phipps JE, Gorpas D, Unger J, Darrow M, Bold RJ, Marcu L. Automated detection of breast cancer in resected specimens with fluorescence lifetime imaging. Phys Med Biol. 2017;63:15003. doi:10.1088/1361-6560/aa983a
20. Shapiro SS, Wilk MB. An analysis of variance test for normality (complete samples). Biometrika. 1965;52(3/4):591–611.
21. Mann HB, Whitney DR. On a test of whether one of two random variables is stochastically larger than the other. Ann Math Stat. 1947:50–60.
22. Breiman L Random forests. Mach Learn. 2001;45(1):5–32.
23. Hecht-Nielsen R Theory of the backpropagation neural network. In: Neural Networks for Perception. Elsevier; 1992:65–93.
24. Cortes C, Vapnik V. Support-Vector Networks. Mach Learn. 1995;20:273–297. doi:10.1109/64.163674
25. Datta R, Garcia Alfonso A, Cinco R, Gratton E. Fluorescence lifetime imaging of endogenous biomarker of oxidative stress. Sci Rep. 2015;5:9848. [PubMed: 25993434]
26. Swatland HJ. Autofluorescence of adipose tissue measured with fibre optics. Meat Sci. 1987;19(4):277–284. [PubMed: 22056049]
27. Pantalone D, Andreoli F, Fusi F, et al. Multispectral imaging autofluorescence microscopy in colonic and gastric cancer metastatic lymph nodes. Clin Gastroenterol Hepatol. 2007;5(2):230–236. [PubMed: 17296531]
28. Unger J, Hebisch C, Phipps JE, et al. Real-time diagnosis and visualization of tumor margins in excised breast specimens using fluorescence lifetime imaging and machine learning. Biomed Opt Express. 2020;11(3):1216. doi:10.1364/boe.381358 [PubMed: 32206404]
29. Marsden M, Weyers BW, Bec J, et al. Intraoperative Margin Assessment in Oral and Oropharyngeal Cancer using Label-free Fluorescence Lifetime Imaging and Machine Learning. IEEE Trans Biomed Eng. 2020.
30. Kim SW, Lee HS, Ahn YC, et al. Near-Infrared Autofluorescence Image-Guided Parathyroid Gland Mapping in Thyroidectomy. Journal of the American College of Surgeons. 2017.

31. Ladurner R, Sommerey S, Al Arabi N, Hallfeldt KKJ, Stepp H, Gallwas JKS. Intraoperative near-infrared autofluorescence imaging of parathyroid glands. Surg Endosc. 2017;31(8):3140–3145. [PubMed: 27844237]

32. Demarchi MS, Karenovics W, Bédat B, Triponez F. Intraoperative autofluorescence and indocyanine green angiography for the detection and preservation of parathyroid glands. J Clin Med. 2020;9(3):830.

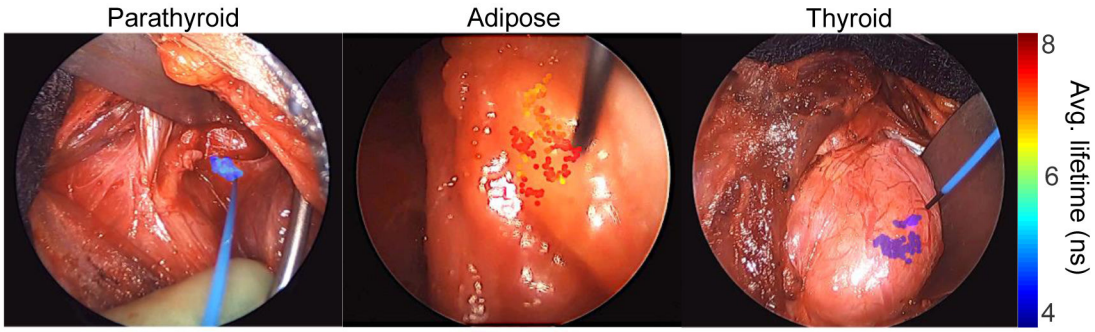

Figure 1: Visualization of measured FLIm data overlaid onto the surgical field of view.
Point-measurements are localized within the surgical field using a blue aiming beam emerging from the fiber probe. Average lifetime values for spectral channel 2 were calculated and then rendered as a at transparent overlay onto the endoscopic image.

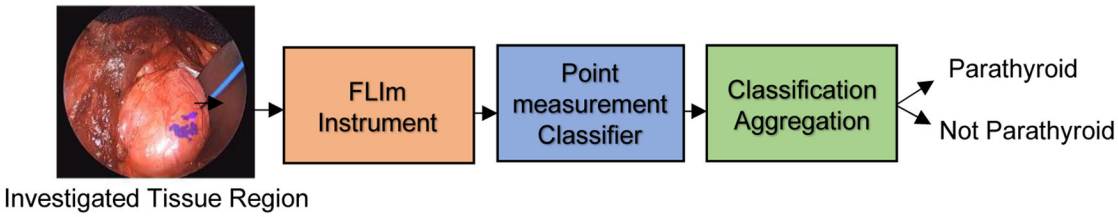

Figure 2: Classification pipeline for FLIm-based parathyroid detection.

N FLIm point-measurements were acquired for a given tissue region to investigate for parathyroid. These N point-measurements were classified using a machine learning model (random forest, support vector machine or neural network) before the N predictions are aggregated together to produce an overall binary prediction through majority voting for the investigated region.

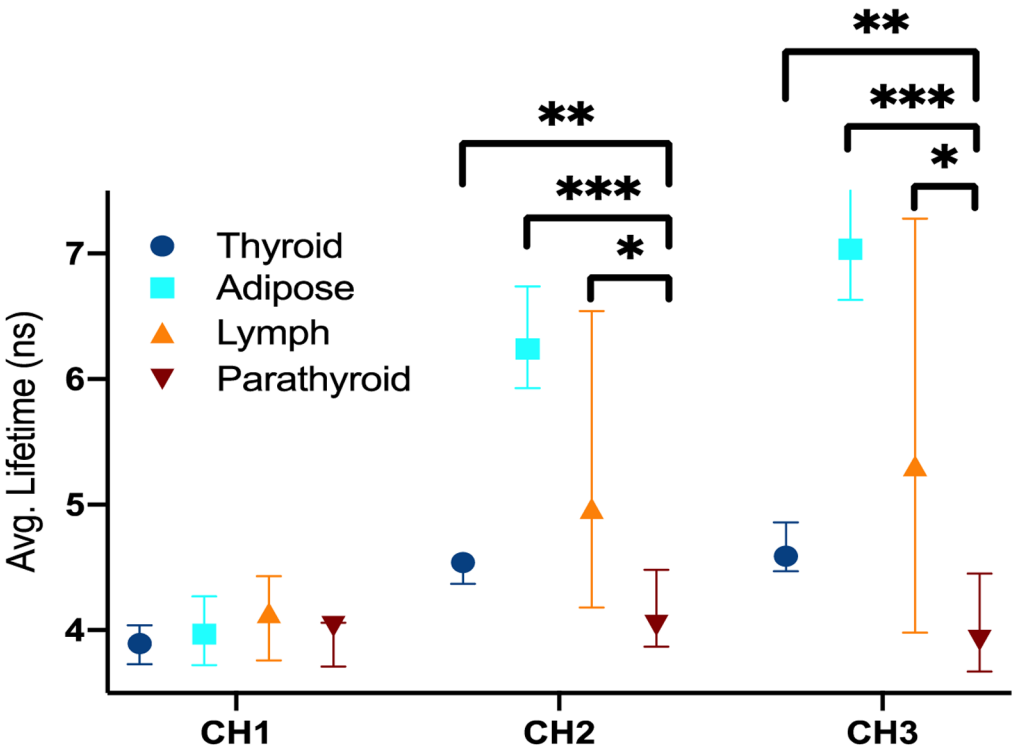

Figure 3: Average fluorescence lifetime for various tissues imaged *in vivo* for N=15 patients.
The lifetimes are displayed for all three spectral channels. A patient level median lifetime was calculated for each tissue type for each patient. The Mann-Whitney U test was performed to check for statistically significant differences between tissue types. * $p<0.05$ ** $p<0.01$ *** $p<0.001$.

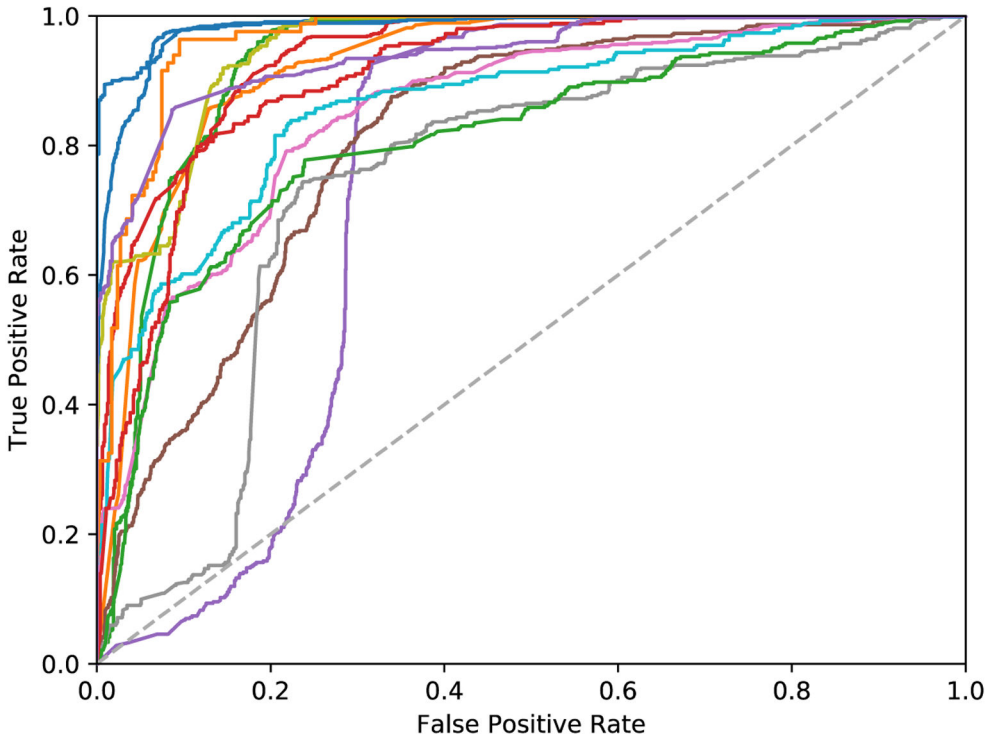

Figure 4: ROC curves for point-measurement level evaluation using the random forests classifier (N=15 patients).

A mean area-under-the-curve (AUC) of 0.88±0.08 was observed, with a minimum AUC of 0.74. The lower performance cases can be attributed to low lifetime lymphoid tissue occasionally being misclassified in certain cases as parathyroid.

Table 1.

Point-measurement level parathyroid classification performance (N=15 patients, 29393 points)

Method	ROC-AUC (±σ)	Sensitivity (%±σ) n=10753	Specificity (%±σ) n=18640
Neural Network	0.90±0.08	64±18	90±8
Support Vector Machine	0.89±0.08	87±10	78±15
Random Forest	0.88±0.08	88±12	71±14

Table 2.

Run-level parathyroid classification performance (N=15 patients, 41 runs)

Method	Sensitivity (%) n=15	Specificity (%) n=26
Neural Network	66	100
Support Vector Machine	76	100
Random Forest	100	93